

Original scientific paper

**MEMS RESONATOR MASS LOADING NOISE MODEL:
THE CASE OF BIMODAL ADSORBING SURFACE AND FINITE
ADSORBATE AMOUNT**

**Ivana Jokić¹, Olga Jakšić¹, Miloš Frantlović¹,
Zoran Jakšić¹, Koushik Guha²**

¹University of Belgrade, Institute of Chemistry, Technology and Metallurgy – National Institute of the Republic of Serbia, Center of Microelectronic Technologies, Belgrade, Serbia

²National MEMS Design Centre, Department of Electronics and Communication Engineering, National Institute of Technology, Silchar, Assam – 788010, India

Abstract. *Modeling of adsorption and desorption in microelectromechanical systems (MEMS) generally is crucial for their optimization and control, whether it is necessary to decrease the adsorption-desorption influence (thus ensuring stable operation of ultra-precise micro and nanoresonators) or to increase it (and enhancing in this manner the sensitivity of chemical and biological resonant sensors). In this work we derive and use analytical mathematical expressions to model stochastic fluctuations of the mass adsorbed on the MEMS resonator (mass loading noise). We consider the case where the resonator surface incorporates two different types of binding sites and where non-negligible depletion of the adsorbate occurs in a closed resonator chamber. We arrive at a novel expression for the power spectral density of mass loading noise in resonators and prove the necessity of its application in cases when resonators are exposed to low adsorbate concentrations. We use the novel approach presented here to calculate the resonator performance. In this way we ensure optimization of these MEMS devices and consequentially abatement of adsorption-desorption noise-caused degradation of their operation, both in the case of micro/nanoresonators and resonant sensors. This work is intended for a general use in the design, development and optimization of different MEMS systems based on mechanical resonators, ranging from the RF components to chemical and biological sensors.*

Key words: *Adsorption, Mass loading noise, Langevin equation, Power Spectral Density, Resonator*

Received March 15, 2021; received in revised form July 07, 2021

Corresponding author: Ivana Jokić

University of Belgrade, Institute of Chemistry, Technology and Metallurgy – National Institute of the Republic of Serbia, Center of Microelectronic Technologies, 11000 Belgrade, Serbia

E-mail: ijokic@nanosys.ihtm.bg.ac.rs

* This paper is loosely based on the authors' invited presentation from the 1st International Conference on Micro/Nanoelectronics Devices, Circuits and Systems (MNDCS 2021), 29 - 31 January, 2021, in Silchar, Assam, India. [1]

1. INTRODUCTION

Compared to the conventional mechanical resonators, micromechanical resonant structures manufactured by MEMS (Microelectromechanical system) or NEMS (Nanoelectromechanical system) technologies have many favorable features. These include their extremely compact dimensions of the order of micrometers or nanometers, the technological compatibility – and thus vastly facilitated integration – with active electronics, low power consumption, an extended range of available resonant frequencies (even reaching the gigahertz range), high reliability and batch production with a high yield and a very low cost per unit element. This makes them convenient for applications in electronics, as frequency defining units of miniature oscillators and frequency selective circuits [1-4]. Additionally, the easy adjustability of their parameters makes them promising candidates for tunable passive components, which further enables reconfigurability, a higher integration degree and miniaturization of radio-frequency circuits [3]. MEMS/NEMS resonators are also being developed for various sensing applications and represent the basic components of highly sensitive resonant sensors of mass, force, acceleration, temperature, as well as the concentration of various chemical substances and biological agents [5-8], often being based on micro- and nanocantilevers.

Smaller device dimensions lead to an increase of the surface-to-volume ratio, which boosts their sensitivity to some physical processes whose effects are negligible in larger structures. Among such processes are adsorption and desorption (AD) of particles from the surrounding medium, which occur at the surface of the structure, and results in varying amounts of mass being added to the native resonator mass, thus changing the resonant frequency of the device. This process enables the operation of AD-based chemical and biological sensors, however in other resonant devices it is undesirable. The added mass randomly fluctuates due to the stochastic nature of the AD processes. In resonators, these fluctuations are known as mass loading noise or resonator AD noise [9]. They contribute to the total frequency noise of the resonator, together with other noise sources (including temperature fluctuations, outgassing, Brownian motion, Johnson (thermal) noise, drive power and self-heating, random vibration, flicker (1/f) noise, etc. [10-12]), and therefore degrade the performance of electronic devices and sensors of which the microresonator is an integral part. It is particularly important to analyze this kind of fundamental noise, since it allows for the optimal resonator design and optimization of the operating conditions, which consequently ensures lower noise levels and, accordingly, minimizes signal degradation in electronic circuitry and improves detection limits in sensors. Based on these facts, there is a need to establish a mathematical model of particles binding-unbinding process at the resonator surface as accurately as possible, enabling the analysis of mass loading noise.

Numerous models of mass loading noise in microresonators, nanoresonators and other micro- and nanostructures applicable to different practical situations can be found in literature [9-10, 13-16]. A majority of them assumes the existence of only one type of binding sites on the adsorbing surface, so that the adsorption and desorption of one species is characterized by one pair of adsorption and desorption rate constants and most often it is described by the Langmuir model. However, usually the real surfaces are not uniform, and each of them is characterized instead by different structural, morphological or chemical features, which results in a difference between its surface adsorption sites. If this is the case, the AD process is characterized by some spatial distribution of AD rate constants across the surface. The simplest type of such surfaces has two distinct kinds of adsorption binding sites, so that there

is a bimodal surface affinity for the particles of a given species. In that case the kinetics of AD processes and resonator noise are described by models that imply a bi-Langmuir AD process [17, 18]. In certain cases it is necessary that the models of AD process and noise include some additional effects which may be of importance. One of such effects is depletion of adsorbate particles in the resonator chamber due to adsorption, which may be significant, especially at low adsorbate concentrations and for small dimensions of the resonator chamber, as described in [19]. The joint effect of the two phenomena to the AD process kinetics has been analyzed in [20], while a model of the dynamics of the equilibrium fluctuations, AD noise in frequency domain, has not been established yet for such a case.

Here we present a new mathematical model of mass loading noise, which is more comprehensive than the other mass loading noise models previously published in the literature, since it simultaneously takes into account the bimodal surface affinity and the decrease of the analyte concentration in a chamber containing the resonator, caused by particles adsorption-desorption processes and the finite dimensions of the chamber. In this way, the model can closely approximate the conditions that exist in practice when resonators are exposed to low adsorbate concentrations.

2. MASS LOADING NOISE MODELING

A bimodal adsorbing surface (illustrated in Fig. 1) implies the existence of two types of binding sites, which differ in their affinity for binding adsorbate particles from the ambient. The adsorption-desorption of adsorbate particles on such a surface is characterized by two pairs of adsorption and desorption rate constants, (k_{f1}, k_{r1}) and (k_{f2}, k_{r2}) , corresponding to the sites of type 1 and 2, respectively. If N_{a1} and N_{a2} are the numbers of binding sites of the two types on the resonator surface, and N_{0t} is the number of particles in the resonator chamber at the moment t , the time evolution of the numbers of particles adsorbed at the sites of the first, N_1 , and of the second type, N_2 , is determined by the equations

$$\frac{dN_1}{dt} = k_{f1}N_{0t}(N_{a1} - N_1) - k_{r1}N_1 \quad (1)$$

$$\frac{dN_2}{dt} = k_{f2}N_{0t}(N_{a2} - N_2) - k_{r2}N_2 \quad (2)$$

It is assumed here that only one adsorbate particle can be bound to a single site of any kind, and that adsorbate particles do not interact among themselves.

In a closed chamber, N_{0t} is changing over time due to the AD process, and it equals $N_{0t} = N_0 - N_1 - N_2$, where N_0 is the number of particles in the chamber at the moment $t = 0$. Then, Eqs. (1) and (2) constitute the system of nonlinear differential equations [20]

$$\frac{dN_1}{dt} = k_{f1}(N_0 - N_1 - N_2)(N_{a1} - N_1) - k_{r1}N_1 = A_1 - D_1 \quad (3)$$

$$\frac{dN_2}{dt} = k_{f2}(N_0 - N_1 - N_2)(N_{a2} - N_2) - k_{r2}N_2 = A_2 - D_2 \quad (4)$$

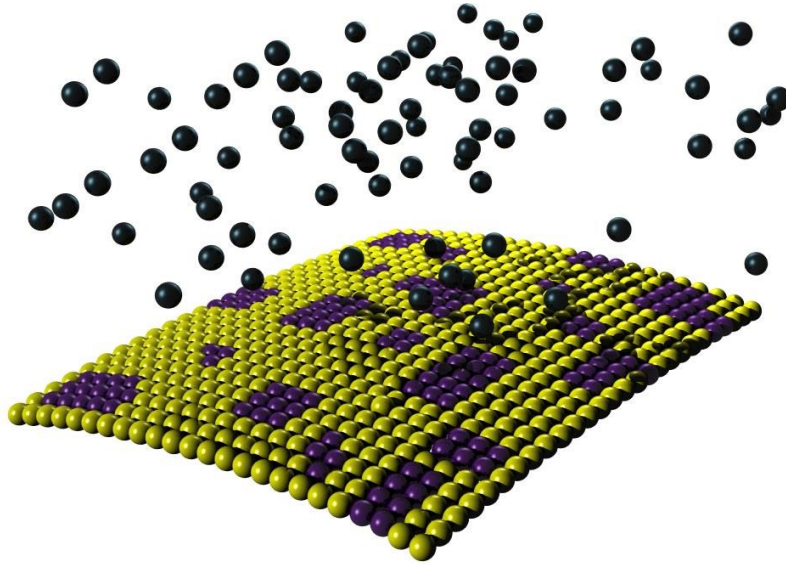


Fig. 1 Illustration of adsorption-desorption process of adsorbate particles on a bimodal surface, characterized by two types of adsorption sites (here represented as surface patches with two different shades).

which is solved numerically for N_1 and N_2 . However, if the numbers of the adsorbed particles in each moment are much smaller than the total number of adsorbate particles in the chamber N_0 , then N_{0t} can be considered constant over time, thus Eqs. (3) and (4) become equal to the equations of the bi-Langmuir model, given by Eqs. (1) and (2) in which $N_{0t} = N_0$. The use of the model that takes into account the adsorbate depletion in the resonator chamber during adsorption, becomes necessary with a decreasing N_0 . Its importance for MEMS resonators becomes obvious since it is known that their use in frequency reference and timing applications requires low operating gas pressures inside the chamber in order to ensure higher Q-factor by minimizing air damping as one of the major energy loss mechanisms [2,3]. Apart from that, micromechanical resonant structures used in adsorption-based chemical and biological sensors also operate under conditions of a small number of adsorbate particles, since these sensors are intended for highly sensitive detection of ultralow analyte concentrations. In both of the given examples, it may not be valid that $N_0 \gg N_1 + N_2$, thus the finite amount of analyte and the depletion over time of the particles available for adsorption should be taken into account when performing the analysis, as predicted by Eqs. (3) and (4).

If M is the mass of a single adsorbate particle, and N is the total number of adsorbed particles, the total adsorbed mass on the resonator surface is

$$m = MN = M(N_1 + N_2) \quad (5)$$

The AD process on the resonator surfaces reaches the steady state after some time. Then the numbers of the adsorbed particles reach the values N_{1e} and N_{2e} , determined by the equations obtained from Eqs. (3) and (4) for $dN_1/dt = 0$ and $dN_2/dt = 0$

$$(K_1 - K_2)N_{1e}^3 + [K_1N_{a2} + K_2N_{a1} - (K_1 - K_2)(N_0 + N_{a1} + K_1)]N_{1e}^2 - [K_1(N_{a2} - N_0) + K_2(2N_0 + N_{a1} + K_1)]N_{a1}N_{1e} + K_2N_0N_{a1}^2 = 0 \quad (6)$$

$$N_{2e} = N_{1e} \frac{K_1N_{a2}}{K_1N_{1e} + K_2(N_{a1} - N_{1e})} \quad (7)$$

Here $K_1 = k_{r1}/k_{f1}$ and $K_2 = k_{r2}/k_{f2}$ are the equilibrium constants.

However, even after reaching the steady state the numbers of adsorbed particles fluctuate due to the inherently random nature of the AD process. These fluctuations result in the fluctuations of the adsorbed mass, known as the mass loading noise, Δm . If ΔN_1 and ΔN_2 denote small fluctuations around the equilibrium values N_{1e} and N_{2e} , the numbers of the adsorbed particles in each moment are $N_1 = N_{1e} + \Delta N_1$ and $N_2 = N_{2e} + \Delta N_2$, and the fluctuations of the adsorbed mass are

$$\Delta m = M\Delta N = M(\Delta N_1 + \Delta N_2) \quad (8)$$

The linear approximation of the functions A_1 , A_2 , D_1 and D_2 (defined in Eqs. (3) and (4)) around the equilibrium values of the adsorbed particles numbers

$$A_{iLA} = A_{ie} + \frac{\partial A_i}{\partial N_1} \Delta N_1 + \frac{\partial A_i}{\partial N_2} \Delta N_2, \quad D_{iLA} = D_{ie} + \frac{\partial D_i}{\partial N_i} \Delta N_i, \quad i=1 \text{ or } i=2 \quad (9)$$

where all the functions and derivatives are calculated for $N_1 = N_{1e}$ and $N_2 = N_{2e}$, enables linearization of Eqs. (3) and (4), which yields the system of Langevin equations after adding an intrinsic source function (ξ_1 and ξ_2) to the right side of each of them

$$\frac{d(\Delta N_i)}{dt} = \left(\frac{\partial A_i}{\partial N_i} - \frac{\partial D_i}{\partial N_i} \right) \Delta N_i + \frac{\partial A_i}{\partial N_j} \Delta N_j + \xi_i, \quad i=1 \text{ or } i=2, j=1 \text{ or } j=2, i \neq j \quad (10)$$

(the equalities $A_{ie} = D_{ie}$ are applied, which stem from the steady-state conditions $dN_i/dt = 0$, for $i = 1$ or $i = 2$). The previous equations may be presented in the form

$$\frac{d(\Delta N_1)}{dt} = -M_{11}\Delta N_1 - M_{12}\Delta N_2 + \xi_1 \quad (11)$$

$$\frac{d(\Delta N_2)}{dt} = -M_{21}\Delta N_1 - M_{22}\Delta N_2 + \xi_2 \quad (12)$$

where

$$\begin{aligned} M_{11} &= k_{r1} + k_{f1}(N_0 + N_{a1} - 2N_{1e} - N_{2e}) & M_{12} &= k_{f1}(N_{a1} - N_{1e}) \\ M_{21} &= k_{f2}(N_{a2} - N_{2e}) & M_{22} &= k_{r2} + k_{f2}(N_0 + N_{a2} - 2N_{2e} - N_{1e}) \end{aligned} \quad (13)$$

Eqs. (11) and (12) have a form suitable for the application of the Langevin procedure to obtain the power spectral density (PSD) of steady-state fluctuations of mass loaded on the resonator, $S_{\Delta m}(f)$, for the case of AD processes of two adsorbates, in the manner presented in [21]. This procedure is performed by solving Eqs. (11) and (12) in the frequency domain in order to obtain the PSD of the fluctuations ΔN_1 and ΔN_2 , denoted as $S_{\Delta N_1}(f)$ and $S_{\Delta N_2}(f)$, and also their cross-spectral density, $S_{\Delta N_1\Delta N_2}(f)$. The PSD of mass loading noise is then, based on Eq. (8)

$$S_{\Delta m}(f) = M^2 S_{\Delta N}(f) = M^2 (S_{\Delta N_1}(f) + S_{\Delta N_2}(f) + 2S_{\Delta N_1 \Delta N_2}(f)) \quad (14)$$

(as derived e.g. in Supplementary data of [15] by using the definition of the spectral density and autocorrelation function of a random variable that equals the sum of two coupled random variables).

After performing all the necessary calculations the result is obtained in the form

$$S_{\Delta m}(f) = S_{\Delta m, LF} \frac{1 + (2\pi f)^2 \tau_3^2}{(1 + (2\pi f)^2 \tau_1^2)(1 + (2\pi f)^2 \tau_2^2)} \quad (15)$$

where

$$\tau_1 = 2 \left[M_{11} + M_{22} + \sqrt{(M_{11} - M_{22})^2 + 4M_{12}M_{21}} \right]^{-1} \quad (16)$$

$$\tau_2 = 2 \left[M_{11} + M_{22} - \sqrt{(M_{11} - M_{22})^2 + 4M_{12}M_{21}} \right]^{-1} \quad (17)$$

$$\tau_3 = \sqrt{(k_{r1}N_{1e} + k_{r2}N_{2e})[(M_{22} - M_{21})^2 k_{r1}N_{1e} + (M_{11} - M_{12})^2 k_{r2}N_{2e}]}^{-1} \quad (18)$$

and the low-frequency magnitude is

$$S_{\Delta m, LF} = 4M^2 (k_{r1}N_{1e} + k_{r2}N_{2e}) \frac{\tau_1^2 \tau_2^2}{\tau_3^2} \quad (19)$$

The characteristic frequencies of the PSD $S_{\Delta m}(f)$ are $f_i = 1/(2\pi\tau_i)$, index i is 1, 2 or 3.

The PSD of resonator frequency noise caused by random mass loading is [10]

$$S_{\Delta v}(f) = \frac{v_0^2}{4m_0^2} S_{\Delta m}(f), \quad (20)$$

where the resonator mass is m_0 , and v_0 is its resonant frequency.

If the analyte depletion due to the adsorption is neglected, Eqs. (1) and (2) become independent and linear. The overall PSD of mass fluctuations is then calculated as the sum of PSDs of mass fluctuations of the both parts of the adsorbed amount (the part adsorbed on the type 1 sites, and the part adsorbed on the other type of sites)

$$S_{\Delta mL}(f) = M^2 S_{\Delta NL}(f) = M^2 (S_{\Delta NL_1}(f) + S_{\Delta NL_2}(f)) = S_{\Delta mL_1}(f) + S_{\Delta mL_2}(f) \quad (21)$$

(this equation stems from Eq. (14) when N_1 and N_2 are statistically independent random variables) and the components 1 and 2 are given by the expression

$$S_{\Delta mL_i}(f) = M^2 S_{\Delta NL_i}(f) = \frac{4M^2 N_{a_i} k_{f_{v_i}} k_{r_i} N_0 / (k_{r_i} + k_{f_{v_i}} N_0)^3}{1 + (2\pi f)^2 / (k_{r_i} + k_{f_{v_i}} N_0)^2}, \quad i=1 \text{ or } i=2 \quad (22)$$

with the characteristic frequency $f_{Li} = 1/(2\pi\tau_{Li})$, where $\tau_{Li} = k_{r_i} + k_{f_{v_i}} N_0$ (i is 1 or 2).

3. RESULTS AND DISCUSSIONS

We investigate the phenomenon of mass loading fluctuations in resonant structures with bimodal surface affinity, influenced by adsorbate depletion from the finite sample during adsorption, as well as quantitatively investigate and compare the results obtained by using the model that takes into account the depletion and the one that neglects it, through the analysis which is as general as possible, i.e. not pertinent to a given micromechanical resonant structure or adsorbate. Therefore, the results of mass loading noise analysis are presented in terms of PSDs of the fluctuations of the total number of adsorbed particles, $S_{\Delta N}(f)$. All the conclusions about $S_{\Delta N}(f)$ easily lead to conclusions about $S_{\Delta n}(f)$ and $S_{\Delta v}(f)$, having in mind the linear relation between their values (Eqs. (14), (20) and (21)). The values of adsorption and desorption rate constants used in the analysis are $k_{f1}=1.3 \cdot 10^{-11}$ 1/s, $k_{r1}=0.4$ 1/s, $k_{f2}=1.3 \cdot 10^{-13}$ 1/s and $k_{r2}=0.02$ 1/s. They belong to the ranges corresponding to biomolecules and biosensors [22, 23], which does not affect the generality of the analysis. The presented results are pertinent to different amounts of adsorbate particles surrounding the resonator (i.e. various adsorbate concentrations or pressures in the chamber of fixed volume). Among a total of $N_a=10^{11}$ adsorption sites on a bimodal affinity surface, different shares of two types of sites are assumed.

Fig. 2 shows the power spectral density of fluctuations of the total number of adsorbed particles according to the model that takes into account adsorbate depletion, $S_{\Delta N}(f)$. It is introduced in Eq. (14), and determined by Eqs. (15)-(19). The same quantity obtained by using the model which assumes a constant adsorbate concentration in the resonator chamber, $S_{\Delta nL}(f)$, given in Eq. (21), is also shown. The concentration of adsorbate in the chamber of volume $1 \cdot 10^{-7}$ m³ is $2.5 \cdot 10^{19}$ 1/m³ (which corresponds to the overall number of adsorbate molecules of $2.5 \cdot 10^{12}$). The equal shares of different types of adsorption sites are assumed ($\nu=0.5$). Also presented on the diagram are the components of $S_{\Delta nL}(f)$, $S_{\Delta nL1}(f)$ and $S_{\Delta nL2}(f)$, that originate from independent fluctuations on the two types of adsorption sites. They are determined by Eq. (22), according to the linear (i.e. bi-Langmuir) model of adsorption on a bimodal adsorbing surface. A good match can be observed between the total PDS values predicted by the two models.

The bi-Langmuir set of equations (1)–(2) models the two adsorbed fractions as independent. Their contributions to the PSD of fluctuations of the total number of adsorbed particles are shown by dashed and dotted lines in the diagram. However, the dynamics of fluctuations of numbers of particles adsorbed on the two types of sites is not actually independent if the adsorbate quantity is finite: although the adsorbate particles independently occupy the two sets of adsorption sites, they deplete the same pool of the free particles. In equilibrium, the surface coverage remains constant on average, but the distribution of the occupied sites continuously changes, with the dynamics determined by the rate constants. The term 'favorable sites' in the analysis refers to the adsorption sites characterized by a greater affinity for the adsorbate (expressed as the ratio of adsorption and desorption rate constants). A greater binding energy will cause the adsorbed particles to reside longer on the surface, hence their desorption rate constant will be lower and there will be less fluctuations at lower frequencies. Truly, in the diagram, at lower frequencies, the fluctuations of the adsorbed fraction with lower rate constants dominate over the fluctuations of the fraction with the greater rate constants (the dashed line is above the dotted line). Naturally, higher rate constants characterize greater dynamics of the process, and at higher frequencies the overall noise level is dominated by the fraction

that exhibits more frequent binding (the dotted line is above the dashed one). After specifying the low frequency noise magnitude (LFNM) and the frequencies at which the PSD curve changes its slope as the characteristic parameters of the PSD, it is of interest to analyze the discrepancy between the two models regarding these parameters over the range of values of concentrations and fractions of favorable sites.

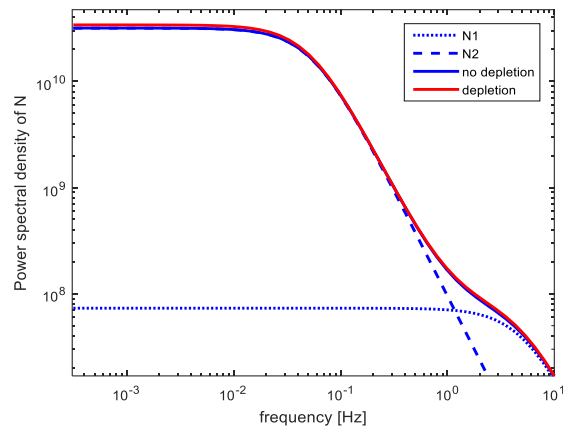


Fig. 2 PSD of the fluctuations of the number of adsorbed particles on the resonator surface (expressed in 1/Hz) with bimodal affinity (for $\nu=0.5$), presented both according to the model that takes into account adsorbate depletion in the resonator chamber, and according to the model that neglects it. The PSDs shown by dotted and dashed lines correspond to the fluctuations of the numbers of particles adsorbed on the two types of sites, N_1 and N_2 , for negligible depletion. The overall number of adsorbate particles is $2.5 \cdot 10^{12}$.

The same quantities as in Fig. 2 are shown in Figs. 3 a-c, but for different adsorbate concentrations: for 5 times (Fig. 3a), 25 times (Fig. 3b) and 50 times (Fig. 3c) lower values. The smaller the concentration, the stronger the depletion of the adsorbate will be in the gas phase and consequently, the greater the discrepancies between the results obtained by the use of the linear model and by the more accurate nonlinear one. In Fig. 3a, a small deviation can be observed between the PSDs of total fluctuations determined according to the two adsorption models. The model that includes adsorbate depletion predicts a slightly higher total noise, and a small difference can also be noticed between the characteristic frequencies of the two spectral densities. Compared to the case shown in Fig. 2, both models at a 5 times lower concentration predict an order of magnitude higher low-frequency noise magnitude, and lower characteristic frequencies. The characteristic frequencies are determined by the parameters τ_1 , τ_2 , τ_3 , τ_{L1} and τ_{L2} , whose values are given in Table 1. A further decrease of the adsorbate concentration results in a significantly higher difference between the PSDs obtained according to the two models, as shown in Fig. 3b.

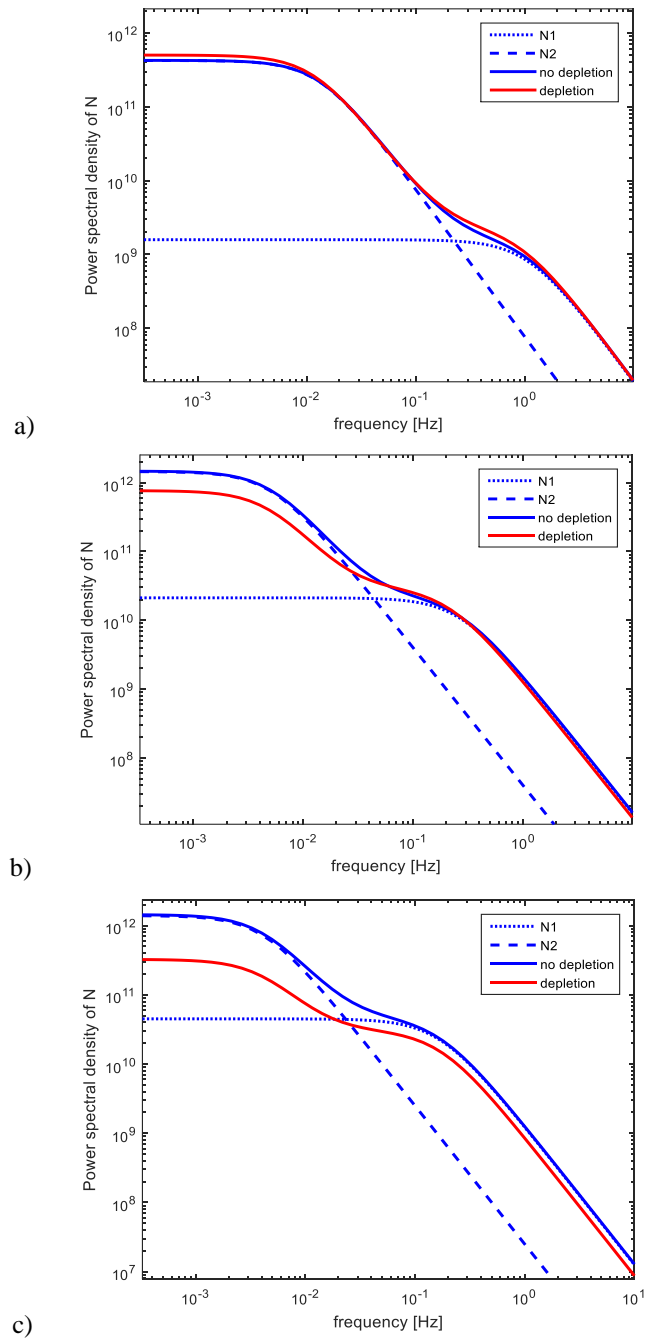


Fig. 3 PSD (expressed in 1/Hz) of the fluctuations of the number of adsorbed particles on a bimodal affinity surface ($\nu=0.5$), according to the two adsorption models for: a) 5 times, b) 25 times, and c) 50 times lower adsorbate concentration than in Fig. 2.

The lower low-frequency noise magnitude is obtained according to the model that takes into account the adsorbate depletion. A certain difference in characteristic frequencies of the spectra can also be observed.

The largest difference between the magnitudes of mass loading noise calculated according to the two models can be observed at the lowest adsorbate concentration used in this analysis (Fig. 3c). The difference exists at all frequencies, so the total noise according to the model that neglects the depletion is higher than that predicted by the more accurate (non-linear) model. However, the difference between the characteristic frequencies of the two spectra is negligible.

Table 1 PSD parameter values of mass loading noise according to the two models for different values of N_0 , i.e. for different cases shown in Figs. 2 and 3 ($\nu=0.5$).

Parameter	Fig. 2	Fig. 3a	Fig. 3b	Fig. 3c
N_0	$25 \cdot 10^{11}$	$5 \cdot 10^{11}$	$1 \cdot 10^{11}$	$0.5 \cdot 10^{11}$
τ_1	0.0316	0.1705	0.7422	0.9346
τ_2	3.0042	13.1688	32.1861	37.6628
τ_3	0.1481	0.8827	6.2486	11.4308
τ_{L1}	0.0304	0.1449	0.5882	0.9524
τ_{L2}	2.8986	11.7647	30.3030	37.7358
Difference between the noise magnitudes	negligible	modest	noticeable	significant

We have seen that the power spectral density is affected by the depletion of the adsorbate in the gas phase due to the adsorption-desorption process. Now we will investigate the influence of the shares of different types of adsorption sites on the surface. Figs. 4 and 5 show the power spectral density for different percentages of the favorable adsorption sites on the surface. Figures 4a-c are obtained for the parameter values which are the same as for Fig. 2, while Figs. 4d-f are obtained for the same parameter values as Fig. 3c, but for three cases: when the favorable sites dominate ($\nu=0.8$), when the unfavorable sites are dominant ($\nu=0.2$), and when the number of different sites is the same ($\nu=0.5$). Figs. 4a-c show a good matching between the two models for all the values of ν , at the same adsorbate concentration ($2.5 \cdot 10^{19} \text{ 1/m}^3$). Therefore, Figs. 4a-c correspond to the systems for which the linear model is applicable. However, Figs. 4d-f, obtained for 50 times lower concentration, show a significant difference between the results according to the two models, for every ν . They demonstrate that for a certain subset of the parameter space the bi-Langmuir model of adsorption does not enable accurate quantification of the noise level, thus the nonlinear model must be applied.

The previous analysis showed that in certain cases the linear model falsely predicts noise levels. The ratio of LFNMs is shown in Fig. 5. It is obtained by dividing the LFNM calculated using the linear model with the LFNM calculated by the nonlinear model. It can be observed that the difference in LFNM is greater for lower adsorbate concentrations. When the difference is significant, it increases with the higher share of the high-affinity sites. Typical concentrations span over a very wide range, and consequently the discrepancy due to the neglected analyte depletion may exceed an order of magnitude.

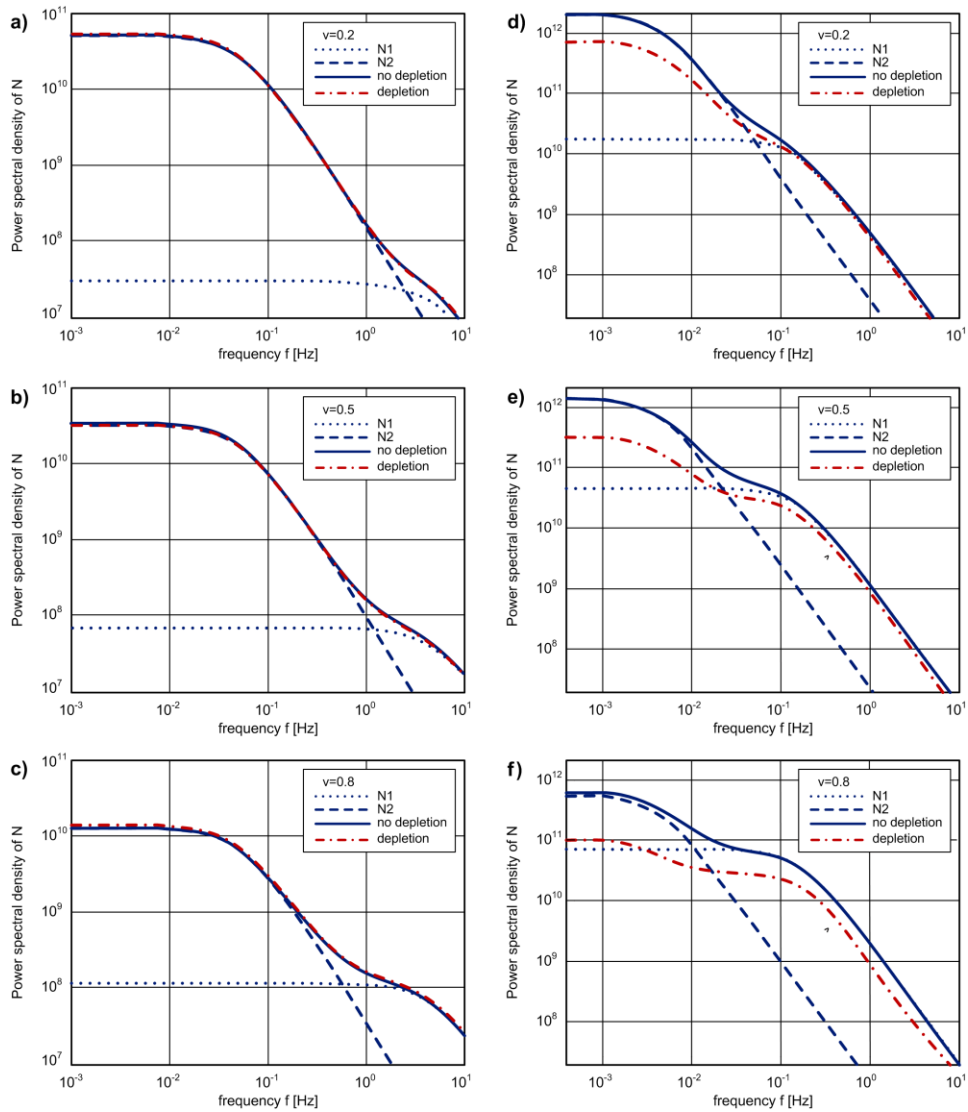


Fig. 4 PSD of the fluctuations of the number of particles adsorbed on a bimodal affinity surface, for different percentages of the favorable adsorption sites, v ($v = 0.2, 0.5, 0.8$), calculated using the model that neglects depletion and the model that takes it into account. The parameters are the same as in Fig. 2 for a-c, and the same as in Fig. 3 c for d-f.

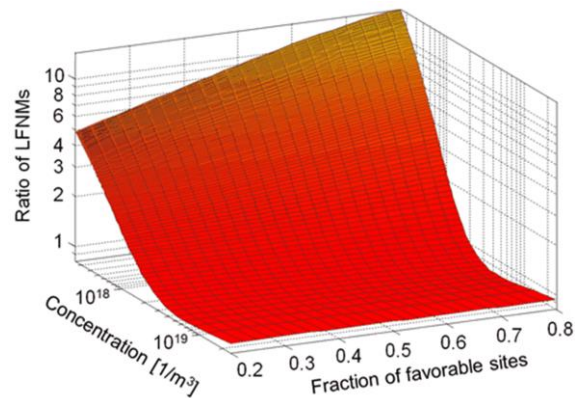


Fig. 5 The ratio of the low frequency noise magnitude (LFNM) calculated by the linear model and the LFNM obtained according to the model that takes into account adsorbate depletion, over the range of adsorbate concentrations and fractions of favorable adsorption sites on the surface.

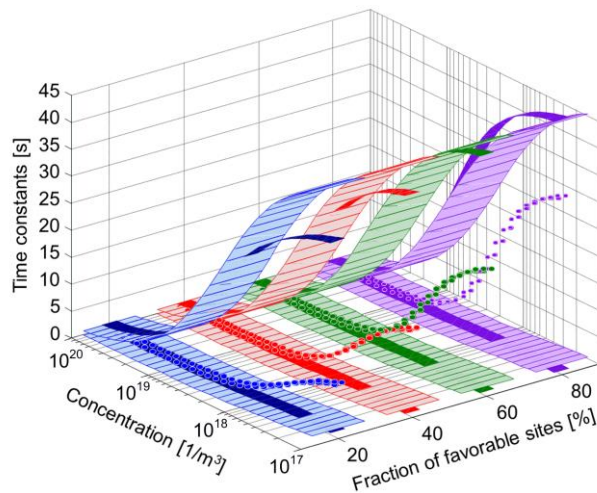


Fig. 6 Time constants calculated by the linear and nonlinear model over a span of adsorbate concentrations and fractions of favorable adsorption sites on the surface. Wide ribbons correspond to τ_{L1} (lower ribbon) and τ_{L2} (upper ribbon) from the linear model, narrow ribbons correspond to τ_1 (lower ribbon) and τ_2 (upper ribbon) from the nonlinear model, while symbols correspond to τ_3 from the nonlinear model. The time constants are calculated for 20%, 40%, 60% and 80% fractions of the favorable sites.

Fig. 6 shows the time constants τ_1 , τ_2 , τ_3 , τ_{L1} and τ_{L2} , which determine the characteristic frequencies of the power spectra according to the two models. The difference between the corresponding characteristic frequencies (i.e. between the time constants τ_1 and τ_{L1} , and also between τ_2 and τ_{L2}) increases with the decrease of the concentration, but the parameter ν also influences the relation between them. The domination of adsorption sites where molecules

bind with lower rate constants (the low percentage of the favorable sites in Fig. 6), does not ensure lower discrepancies between the time constants obtained by the linear and the nonlinear model at low concentrations. Depending on both the concentration and the value of ν , the characteristic frequencies according to the nonlinear model can be higher or lower than the corresponding frequencies predicted by the linear model. However, in the whole examined parameter space they are of the same order of magnitude.

4. CONCLUSION

We presented the results of the stochastic analysis of adsorption-desorption (AD) processes on a micromechanical resonator surface with a bimodal affinity. It is assumed that a resonator operates in an ambient containing a finite and low amount of adsorbate, so there is a significant change of adsorbate concentration in the resonator chamber during adsorption. Such conditions are met e.g. in resonators used in frequency reference and clocking applications, as well as in resonant micromechanical sensors of various physical parameters, chemical substances or biological agents.

The expressions for the power spectral density (PSD) of fluctuations of the number of adsorbed particles are derived by taking into account the adsorbate depletion in the resonator chamber, and also when the depletion is neglected. They yielded the corresponding expressions for the PSDs of mass loading noise, and also for the PSDs of resonator frequency noise.

The analysis was performed by using the computer simulations, based on the two presented noise models. It revealed the change of the discrepancies between the two models in low-frequency noise magnitudes and characteristic frequencies of the noise spectra as the adsorbate amount decreases, and also with the change of the shares of different types of adsorption sites on the resonator surface. All the results and conclusions stemming from the analysis expand the knowledge about the mass loading noise of resonators operating in a closed chamber.

Our results are useful for the estimation of the resonator mass loading noise and the corresponding frequency noise. Additionally, the development of noise models leads to a better understanding of the influence of the resonator parameters and their operating conditions, enabling their optimized design and application, and thus ensuring lower noise levels, minimization of signal degradation in electronic circuits, and improved detection limits in sensors.

The described approach is generally applicable to micro/nanoelectromechanical systems with bimodal affinity surfaces, since each real structure will be exposed to some kind of ambient, and thus to adsorption and desorption of the species present therein. This will be the cause of mass loading effects, including stochastic frequency fluctuations in resonators.

The presented results are pertinent to surfaces with bimodal affinity towards adsorbate particles. However, the described procedure is applicable with simple modifications to the more general case of adsorption on surfaces with multimodal affinity. Hence, our future research will include stochastic analysis of AD processes on surfaces with multimodal affinity towards the adsorbate in trace amounts, with special concern on the interplay between the analyte concentration, the fraction of adsorption sites with different affinities, and the level of influence of the analyte depletion caused by adsorption.

Acknowledgement: *This research was financially supported by the Ministry of Education, Science and Technological Development of the Republic of Serbia, grant number 451-03-9/2021-14/200026.*

REFERENCES

- [1] I. Jokić, M. Frantlović, O. Jakšić, Z. Jakšić, K. Guha, "Mass Loading Noise in Micromechanical Resonators: A Model Considering Bimodal Surface Affinity and Adsorbate Depletion in the Resonator Chamber", 1st International Conference on Micro/Nanoelectronics Devices, Circuits and Systems (MNDCS 2021), 29 - 31 January, 2021, Silchar, Assam, India.
- [2] G. Wu, J. Xu, E.J. Ng, W. Chen, "MEMS Resonators for Frequency Reference and Timing Applications", *J. Microelectromech. Sys.* vol. 29, pp. 1137–1166, September 2020.
- [3] I. Jokić, M. Frantlović, Z. Djurić, M.L. Dukić, "RF MEMS/NEMS resonators for wireless communication systems and adsorption-desorption phase noise", *FU Elec. Energ.*, vol. 28, pp. 345–381, 2015.
- [4] K. Guha, H. Dutta, J. Sateesh, S. Baishya, K. S. Rao, "Design and analysis of perforated MEMS resonator", *Micros. Technol.*, vol. 27, pp. 613–617, November 2021.
- [5] T. Kose, K. Azgin T. Akin, "Design and fabrication of a high performance resonant MEMS temperature sensor", *J. Micromech. Microeng.*, vol. 26, pp. 045012, March 2016.
- [6] S. X. P. Su, H. S. Yang, A. M. Agogino, "A resonant accelerometer with two-stage microleverage mechanisms fabricated by SOI-MEMS technology", *IEEE Sensors J.*, vol. 5, pp. 1214–1223, November 2005.
- [7] R. G. Azevedo, D. G. Jones, A. V. Jog, B. Jamshidi, D. R. Myers, L. Chen, X-a. Fu, M. Mehregany, M. B. J. Wijesundara, A. P. Pisano, "A SiC MEMS resonant strain sensor for harsh environment applications", *IEEE Sensors J.*, vol. 7, pp. 568–576, March 2007.
- [8] F. M. Battiston, J-P. Ramseyer, H. P. Lang, M. K. Baller, C. Gerber, J. K. Gimzewski, E. Meyer, H-J. Güntherodt, "A chemical sensor based on a microfabricated cantilever array with simultaneous resonance-frequency and bending readout". *Sens. Act. B*, vol. 77 pp. 122–131, June 2001.
- [9] Z. Djurić, O. Jakšić, D. Randjelović, "Adsorption-Desorption Noise in Micromechanical Resonant Structures", *Sens. Act. A*, vol. 96, pp. 244–251, February 2002.
- [10] J.R. Vig, "Noise in Microelectromechanical System Resonators", *IEEE Trans. Ultrason., Ferroel. Freq. Contr.*, vol. 46, pp. 1558–1565, November 1999.
- [11] Z. Djurić, "Mechanisms of noise sources in microelectromechanical systems", *Microel. Reliab.*, vol. 40, pp. 919–932, May 2000.
- [12] Y. Nie, H. Zhan, Z. Zheng, A. Bo, E. Pickering, Y. Gu, "How Gaseous Environment Influences a Carbon Nanotube-Based Mechanical Resonator", *J. Phys. Chem. C*, vol. 123, pp. 25925–25933, October 2019.
- [13] C Mathai, SA Bhawe, S Tallur, "Modeling the colors of phase noise in optomechanical oscillators", *OSA Continuum*, vol. 2, pp. 2253–2259, July 2019.
- [14] Z. Djurić, I. Jokić, M. Frantlović, O. Jakšić, "Fluctuations of the number of particles and mass adsorbed on the sensor surface surrounded by a mixture of an arbitrary number of gases", *Sens. Act. B*, vol. 127, pp. 625–631, November 2007.
- [15] M. Frantlović, I. Jokić, Z. Djurić, K. Radulović, "Analysis of the Competitive Adsorption and Mass Transfer Influence on Equilibrium Mass Fluctuations in Affinity-Based Biosensors", *Sens. Act. B*, vol. 189, pp. 71–79, December 2013.
- [16] O. Jakšić, Z. Jakšić, Ž. Čupić, D. Randjelović, L. Kolar-Anić, "Fluctuations in transient response of adsorption-based plasmonic sensors", *Sens. Act. B*, vol. 190, pp. 419–428, January 2014.
- [17] I. Jokić, O. Jakšić, M. Frantlović, Z. Jakšić, K. Guha, "Influence of sensing surface bimodal affinity on biosensor steady-state response", In Proceedings of the 9th Internat. Conf. on Defensive Technologies OTEH, Belgrade, pp. 106.1–4, October 2020.
- [18] T. Contaret, J.-L. Seguin, P. Menini, K. Aguir, "Physical-Based Characterization of Noise Responses in Metal-Oxide Gas Sensors", *IEEE Sensors J.*, vol. 13, pp. 980–986, Nov. 2013.
- [19] I. Jokić, O. Jakšić, "A second-order nonlinear model of monolayer adsorption in refractometric chemical sensors and biosensors case of equilibrium fluctuations", *Opt. Quant. Electron.*, vol. 48, pp. 1–7, June 2016.
- [20] I. Jokić, O. Jakšić, M. Frantlović, Z. Jakšić, K. Guha, K.S. Rao, "Temporal response of biochemical and biological sensors with bimodal surface adsorption from a finite sample", *Microsys. Technol.*, October 2020.
- [21] Z. Djurić, I. Jokić, M. Frantlović, O. Jakšić, D. Vasiljević-Radović, "Adsorbed Mass and Resonant Frequency Fluctuations of a Microcantilever Caused by Adsorption and Desorption of Particles of Two Gases", In Proceedings of the 24th Internat. Conf. on Microel. MIEL, vol. 1, pp. 197–199. Niš, Serbia, May 2004.
- [22] G. Canziani, W. Zhang, D. Cines, A. Rux, S. Willis, G. Cohen, R. Eisenberg, I. Chaiken, "Exploring Biomolecular Recognition Using Optical Biosensors", *Methods*, vol. 19, pp. 253–269, May 1999.
- [23] D.G. Myszkka, X. He, M. Dembo, T.A. Morton, B. Goldstein, "Extending the Range of Rate Constants Available from BIACORE: Interpreting Mass Transport-Influenced Binding Data", *Biophys. J.*, vol. 75, pp. 583–594, August 1998.